Aeidapu Mahesh[1] / Kanwarjit Singh Sandhu[2]

Optimal Switching Angle Scheme for a Cascaded H Bridge Inverter using Pigeon Inspired Optimization

[1] Department of Electrical Engineering, National Institute of Technology, Kurukshetra, Haryana, India, E-mail: mahesh.aeidapu@gmail.com
[2] Department of Electrical Engineering, National Institute of Technology, Kurukshetra, Haryana, India, E-mail: kjssandhu@rediffmail.com

Abstract:
This paper presents an approach using Pigeon Inspired Optimization (PIO) for selective harmonic elimination in a cascaded H-bridge (CHB) multilevel inverter fed with unequal dc sources. The aim of this work is to find the optimal combination of switching angles, such that the lower order harmonics are eliminated and the output voltage is constant irrespective of voltage change in the input side. This paper the PIO has been used to find the optimal angles for a 7-level inverter and the method can be scaled to any number of levels. To show the effectiveness of PIO the results have been compared with other evolutionary algorithms such as genetic algorithm (GA), particle swarm optimization (PSO). An adaptive switching angle strategy has also been developed using ANN to make the proposed strategy suitable to the real-time applications. In order to verify the results, an experimental prototype of 7 level CHB has been developed in the laboratory using dSPACE ds1104 R&D controller board. The results show that the PIO is the most accurate and fastest evolutionary algorithm for switching angle optimization and the experimental results are in close agreement with the simulation results.

Keywords: switching angle optimization, Pigeon inspired optimization, Cascaded H-bridge Inverter

DOI: 10.1515/ijeeps-2017-0205

Received: September 18, 2017; **Revised:** December 5, 2018; **Accepted:** December 10, 2018

1 Introduction

The multi-level inverters have been used widely in the industry for medium voltage and higher power applications due to their advantages such as higher efficiency, lower switching losses, and good electromagnetic compatibility than the two-level inverter. Due to the presence of several levels of DC voltages, the output waveform is synthesized to match the sinusoidal waveform. With the modular structure and simplicity of control, the cascaded H-bridge (CHB) voltage source inverters are particularly more attractive than the other inverter topologies such as the Diode-clamped inverter and flying capacitor inverter.

The cascade H-bridge multi-level inverter (CHB-MLI) is also more suitable for the renewable energy sources such as solar photovoltaic (PV) systems, where each panel or series/parallel connected PV panels act as an isolated DC source for each bridge and output staircase voltage will be the combined voltage of all the bridges. This can also eliminate the need of the transformer to step-up the voltage as number of bridges can be added in cascade to produce the required output voltage level.

Total harmonic distortion (THD) minimization is the important design consideration of any MLI. Various control strategies and optimization strategies have been proposed in the literature for minimizing the output THD. The selective harmonic elimination (SHE) has been used for the elimination of of selected number of harmonics is presented in [1]. Another method of eliminating lower order harmonics has been proposed by using Newton-Raphson (N-R) method in [2, 3]. But, N-R methods requires a good initial guess, without which the solution does not converge. Further, solving of such non-linear transcendental equations is a lot of computational burden, which will take a lot of time. To generate a desired output by reducing the effect of higher order harmonics a method based on the theory of symmetrical polynomials has been proposed in [4], however the number of switching angles is limited to six only. Further, the deterministic and stochastic methods are also been used in [5] and also the curve fitting is also used in [6] to solve the SHE equations in the literature.

The evolutionary optimization algorithms have also been used by various authors in the literature. A genetic algorithm based optimization method to eliminate higher order harmonics and also to maintain constant value

Aeidapu Mahesh is the corresponding author.

of fundamental output voltage is proposed in [7]. However, the proposed method has a limitation over the modulation index value for a wide range. Another method based on GA, simulated annealing (SA) and generalized pattern search has been used in [8]. The Bee swarm optimization for the optimization of the switching angles is proposed in [9]. Further, the other evolutionary optimization methods such as PSO [10, 11], Combination of PSO and harmony search [12] are proposed in the existing literature.

The Artificial neural networks (ANN) has also been used in [13, 14] to measure the switching angles optimally to reduce the output THD. A graphic search method has been adopted in [15] to eliminate the lower order harmonics. Another method based on a polynomial homotopy continuation (PHC) algorithm based algorithm has been used to solve this unified SHE equations in [16]. A new power sharing algorithm along with the SHE-PWM has been proposed in [17]. A comprehensive review of the various evolutionary algorithms used for the harmonic minimization is presented in [18, 19].

In this paper, the PIO, which is a relatively new optimization technique has been used for switching angle optimization for a CHB-MLI with un-equal input DC voltages, which will make it suitable for the PV based applications. The PIO is a much faster and robust algorithm when compared to their counterparts such as GA, PSO. Once the optimized firing angles are obtained over different combinations of input voltages, then the data has been used to train the ANN, which will produce the switching angles in real time. The simulation results are compared with the other methods and an experimental setup has also been developed to confirm the feasibility of the proposed strategy.

The rest of the paper is organized as follows. Sections 2 and 3 explain about the basic operation of the cascaded H-bridge inverter and CHB with unequal dc voltage sources. The PIO has been explained in Section 4 and the proposed strategy has been explained in Section 5. The Section 6 talks about the simulation results and the comparison with the other evolutionary methods. The experimental results are shown in Section 7. The ANN based adaptive switching angle strategy has been presented in section 8 and finally, the concluding remarks have been presented.

2 Cascaded H-bridge inverters

The topology of a single phase 7-level cascaded H-bridge (CHB) inverter is shown in Figure 1. It consists of three H-bridge (single phase full bridge inverter) cells in series and each of the bridge can generate three voltage levels: $+V_{dc}$, 0, $-V_{dc}$. In total, the output stair-case voltage will contain $2S + 1$ levels, where S is the number of H-bridge cells and number of dc sources. When three H-bridges are connected in series the output voltage waveform will have 7 levels as shown in the figure. The basic advantages of this topology are; modular structure, easy protection, and easy modulation control. But, unlike the other topologies like the diode-clamped bridge, this CHB inverter require isolated DC sources for each bridge.

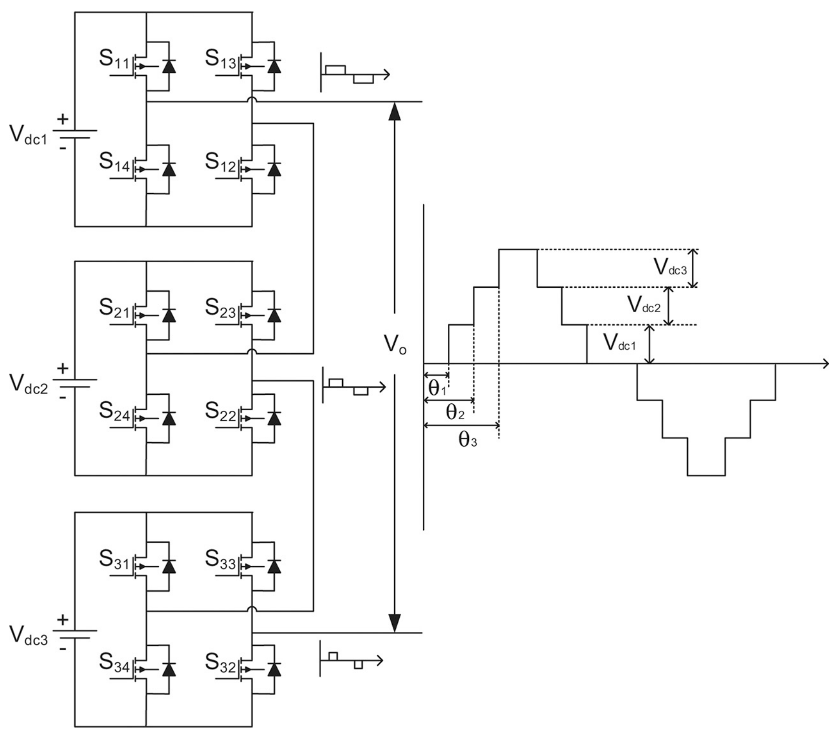

Figure 1: 7-level cascade H-bridge inverter.

The square wave modulation at the power frequency has been used for this structure, in order to obtain lower switching losses. Apart from that, it is simple and easy to implement with this structure.

2.1 Selective harmonic elimination

The selective harmonic elimination pulse width modulation (SHE-PWM) is one of the very common method to eliminate the lower order harmonics from the output of the CHB-MLI. The major advantage of the SHE over the other PWM techniques is that the switching losses are very low as the devices need to be switched only twice during a switching cycle. In this method the three independent angles for each bridge can be used to eliminate two harmonics in the phase voltage and also provide an adjustable modulation index, defined by the following equations,

$$cos(\theta_1) + cos(\theta_2) + cos(\theta_3) = 3m \tag{1}$$

$$cos(5\theta_1) + cos(5\theta_2) + cos(5\theta_3) = 0 \tag{2}$$

$$cos(7\theta_1) + cos(7\theta_2) + cos(7\theta_3) = 0 \tag{3}$$

By solving the above equations, a combination of switching angles can be obtained, which will be producing the output voltage without 5th and 7th harmonics in it.

But, when the CHB-MLI is fed with un-equal DC sources, the harmonic elimination strategy using the SHE-PWM will not result into the feasible solutions because of the increase in the number of unknown variables. This kind of phenomenon can occur when each of the CHB cell is fed by the different PV panels, where the output voltage from each of the panel will be different, due to various factors such as dusting, ice-formation or partial shading due to clouds or trees.

3 CHB inverter with unequal dc sources

In many practical applications, there is a possibility that the input isolated dc sources are not constant and equal for each and every time. One such application is the CHB fed by the PV panels in place of constant dc sources. The Figure 2 shows the P-V curve of the PV panel under varying value of irradiation from 0.2 p.u. to 1 p.u. From the figure it can be seen that the value of V_{mpp} is also varies from 25 V to 27 V for the given range of irradiation values. So, from this curve, it can be observed that the output voltage from a PV panel varies with irradiation to get the maximum power output from the panel. Moreover, for each H-bridge cell, there will be multiple panels connected in series, which will result into considerable variation in the input voltage of the inverter. If ΔV is the voltage variation caused by single panel, if N_s number of panels connected in series then the variation in the voltage is given by

$$\Delta V_T = N_s * \Delta V \tag{4}$$

Due to this varying input voltages, both the output voltage rms value and the shape of the output voltage waveform is always varying, resulting into the poor quality of power produced from the system which is a completely undesirable situation.

By the Fourier analysis, the output staircase waveform for the unequal dc-voltages can be expressed as

$$V(\omega t) = \sum_{n=1,3,5...}^{\infty} \frac{4V_{dc}}{n\pi}(K_1 cos(n\theta_1) + K_2 cos(n\theta_2) + K_3 cos(n\theta_3)) \cdot sin(n\omega t) \tag{5}$$

where, $K_s V_{dc}$ gives the individual DC input voltage of the three DC sources and θ_1, θ_2, θ_3 are their respective switching angles.

The equation (5) expresses the output voltage as the sum of fundamental and odd harmonics. And when the input voltages are varying in nature, it is desirable to maintain the fundamental component of the output voltage constant and eliminate lower order non-triplen odd harmonics in this case 5^{th} and 7^{th}. To equations pertaining to fundamental and odd harmonics are given by,

$$V_{fund} = \frac{4V_{dc}}{\pi}(K_1 cos(\theta_1) + K_2 cos(\theta_2) + K_3 cos(\theta_3)) \tag{6}$$

$$V_5 = \frac{4V_{dc}}{5\pi}(K_1 cos(5\theta_1) + K_2 cos(5\theta_2) + K_3 cos(5\theta_3)) \tag{7}$$

$$V_7 = \frac{4V_{dc}}{7\pi}(K_1 cos(7\theta_1) + K_2 cos(7\theta_2) + K_3 cos(7\theta_3)) \tag{8}$$

To solve this issue, in this paper a methodology has been adopted to find the optimal switching angles, which would produce the minimum value of the THD and at the same time maintain the output voltage at a desirable level. For achieving this an optimization problem has been developed and the respective constraints are also developed.

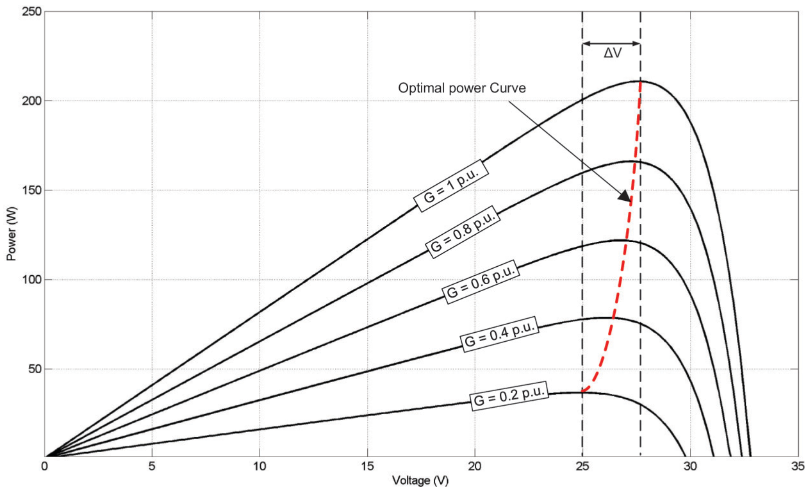

Figure 2: P-V curve of a PV panel with varying irradiation values.

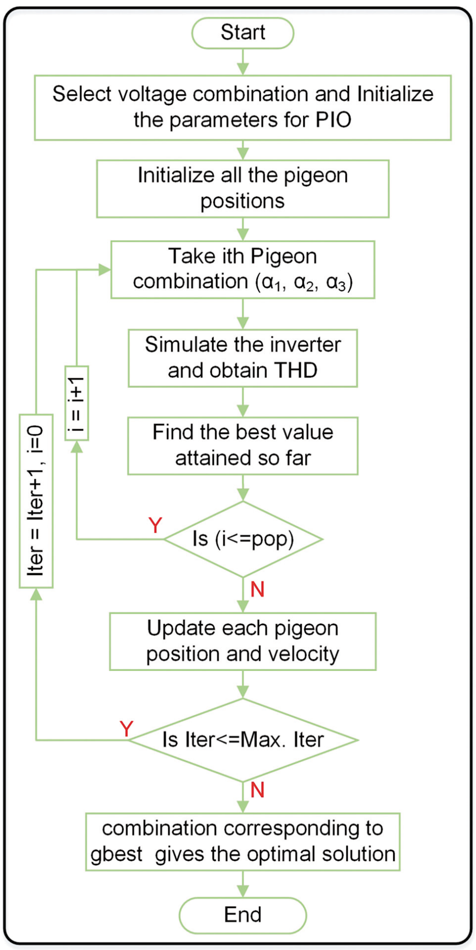

Figure 3: Flow chart of the proposed strategy using PIO.

4 Pigeon inspired optimization

The pigeons are the special species which exhibits the special behavior called homing. Due to this feature, the pigeons have been widely used in World War II for communication purpose. Based on three factors, the pigeons can find their way back are the sun, the earth's magnetic field and the landmarks. Based on the earth's magnetic field they can locate themselves relative to the destination and based on the sun's altitude they find the direction to move. These to features have been modeled into an operator called as the map & compass operator and the other operator is called the landmark operator.

In a d-dimensional space, a set of pigeon positions are randomly generated with initial velocities. Then after their fitness values will be calculated and the best of the finess vlaue is called as the G_{best}. Then for the rest of the iterations, the pigeon positions and velocities are updated using,

$$V_i(t) = V_i(t-1)e^{-Rt} + rand.(G_{best} - X_i(t-1)) \tag{9}$$

$$X_i(t) = X_i(t-1) + V_i(t) \tag{10}$$

where R denotes the map & compass factor, *rand* is a random number generated between 0 and 1.

As the Pigeons approach the destination, they use landmark operator instead of the map & compass operator. Few Pigeons can identify the landmarks, so they can directly fly to the destination and the other Pigeons which doesn't know the landmarks will follow them. So, the landmark operator comes into effect, after a chosen number of iterations t_c is reached. In this operator, half of the pigeons which are nearer to the present G_{best} are taken and their center is found using,

$$N_P(t) = \frac{N_P(t-1)}{2} \tag{11}$$

$$X_c(t) = \frac{\sum X_i(t) \cdot fitness(X_i(t))}{N_P \sum fitness(X_i(t))} \tag{12}$$

Once, the population has been divided into half and their center has been found, then the position updation rule changes to,

$$X_i(t) = X_i(t-1) + rand \cdot (X_c(t) - X_i(t-1)) \tag{13}$$

At the end of the total number of iterations, the pigeon with optimum objective function value will be the global optimum value for the problem. The PIO algorithm has very fast convergence rate, when compared to the other evolutionary algorithms and also successfully implemented for entry guidance of reentry vehicles [20] and pathfinding [21] applications.

5 Proposed strategy

To eliminate the lower order harmonics and also to maintain the fundamental constant the following objective function has been chosen in this work,

$$f(V_{fund}, V_5, V_7) = w_1 * |V_{fund} - V_{ref}| + w_2 * |V_5| + w_3 * |V_7| \tag{14}$$

while satisfying the following constraints,

$$0 < \theta_1 \leq \pi/2 \tag{15}$$

$$0 < \theta_2 \leq \pi/2 \tag{16}$$

$$0 < \theta_3 \leq \pi/2 \tag{17}$$

$$V_{fund} - V_{ref} \leq \epsilon \tag{18}$$

where, V_{ref} is the desired reference voltage, ε is the acceptable error tolerance and w_1, w_2, and w_3 are the weights for each component in the objective function. For this study, the V_{ref} is taken as 110 V and the ε is 1 V, i.e. a small fluctuation in the fundamental voltage between 110 to 111 V is acceptable for a solution.

The proposed strategy for finding the optimal switching angles using PIO is as shown in the Figure 3. Initially, a set of dc voltages V_{dc1}, V_{dc2}, V_{dc3} have been chosen and then PIO is implemented. At first, the initial population is randomly generated over the entire search space i.e. each combination of $\{\theta_1, \theta_2\theta_3\}$ which will give us a particular value of THD is treated as a pigeon in the search space. Then the best value of all of the pigeons is identified and marked as g_{best} and the respective positions (angles) are also stored as the best solution attained so far. Then after, the pigeon positions are updated by using the velocity eq. (9). Then the same process will be repeated for identifying the best pigeon in the population. Further, the landmark operator can also be used for updating the position of the pigeons after certain number of iterations, but, it has not been considered in this paper as the PIO is able to converge to the optimal value in few iterations only. An optimal switching angle combination (θ_1, θ_2, θ_3) will be found with minimum THD at the end of the simulation while satisfying the constraints as given above. Similarly, for each different combination of input voltage, the optimal switching angles can be found by repeating the above strategy.

6 Simulation results

The simulation study for the proposed strategy has been carried out in MATLAB/Simulink environment. A 7-level CHB has been modeled in Simulink and the optimization using PIO has been developed as an m-file. For this study, the voltages have been randomly varied in steps of 1 V, ([50,50,50],[50,50,51]...[60,60,60]) to generate different combinations. The parameters used for the PIO algorithm are tabulated in Table 1.

Table 1: Parameters used for PIO.

Parameter	Value
population size	50
Map & compass factor (r)	0.2
Maximum iterations	50

In order to show the effectiveness of PIO when compared with the other competitive evolutionary algorithms, the same voltage combinations are also simulated using PSO and GA as well. To maintain the proper comparison among all the algorithms, the general parameters such as the population size and the number of iterations are kept same for all the algorithms and the remaining parameters are chosen as per the requirement of the algorithm and are tabulated in Table 2 and Table 3. The simulation results obtained for 20 randomly generated voltage combinations are presented in Table 4.

Table 2: Parameters used for PSO.

Parameter	Value
population size	50
Acceleration constants (C_1&C_2)	1.4 & 2.6
Inertia constants (W_{max}&W_{min})	1.0 & 0.4
Maximum iterations	50

Table 3: Parameters used for GA.

Parameter	Value
Population Size	50
Maximum Generation	50

Crossover probability	0.9
Mutation probability	0.005
Elitism probability	0.1

From the results, it can be seen that the minimum THD for each case has been obtained by using PIO only and the others have a bit higher value of THD for most of the cases. And the other important observation is that the PIO require only fewer iterations to find the optimal solution when compared to the other optimization methods. The Figure 4 indicates that the PIO takes only 10 iterations to reach the globally optimal solution, while the other algorithms PSO and GA have taken more number of iterations. So, from the above results, it can be clearly seen that the PIO is able to achieve the global optimum within a very short period of time when compared to the other algorithms.

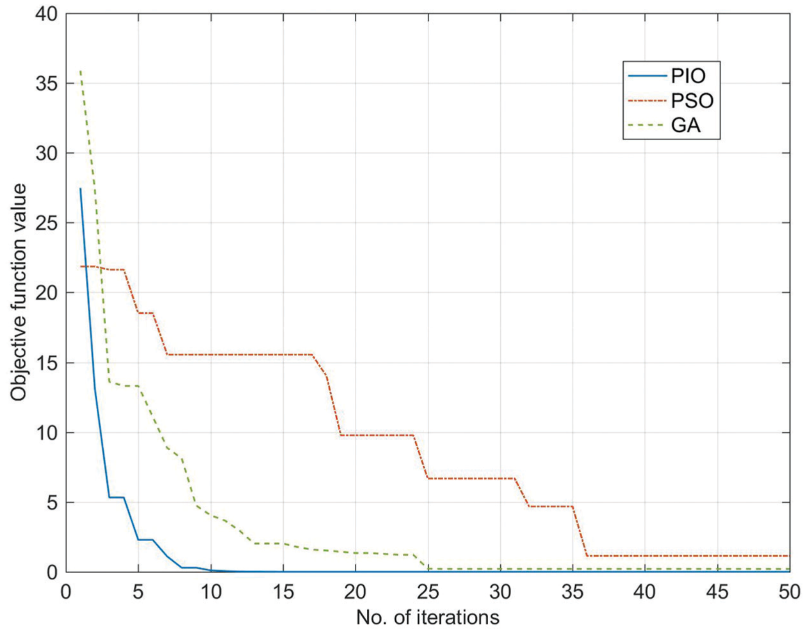

Figure 4: Comparison for the speed of different algorithms.

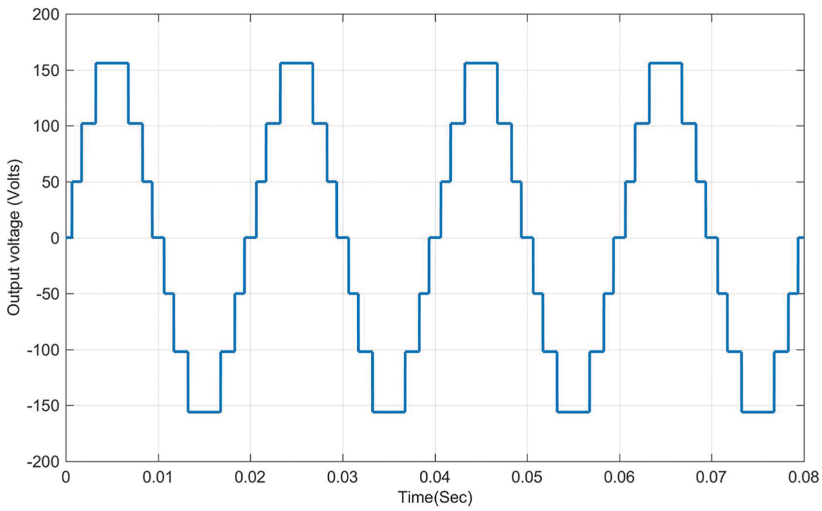

Figure 5: Output voltage waveform for $V_{dc1} = 59$, $V_{dc2} = 55$, $V_{dc3} = 60$.

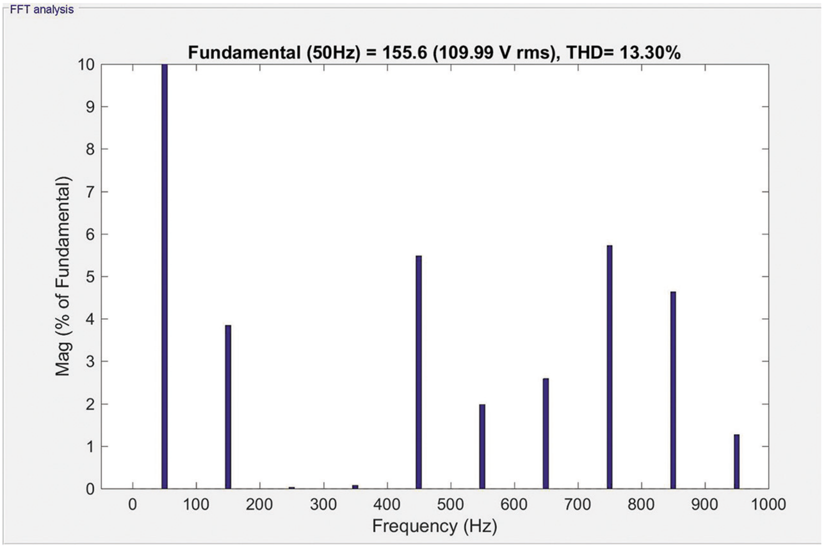

Figure 6: THD spectrum for $V_{dc1} = 59$, $V_{dc2} = 55$, $V_{dc3} = 60$.

As all the algorithms used in this work are heuristic in nature, there is always a possibility of getting stuck in the local optima for a particular algorithm. But, in order to ensure that the algorithms are reaching the global optimum, the algorithms have been run repeatedly for the same input and verified that whether they are converging to the global minimum or not. The result of such repetition operation has been given in the form of Table 5. The same input has been given to all the algorithms and 10 consecutive runs for each algorithm have been performed and the number of function calls each algorithm to reach the designated global optimum have been obtained. And from this result also indicates that the PIO was able to repeat the same solution every time and the average number of function calls it has to make is considerably less when compared to the other algorithms. The time taken for each function call is computed on a computer running on an Intel Core - i7 processor @ 3.6 GHz clock frequency and 4 GB RAM.

Table 4: Simulation results for different voltage combinations and different optimization techniques.

S. No.	Voltages			PIO				PSO				GA			
	V_{dc1}	V_{dc2}	V_{dc3}	θ_1	θ_2	θ_3	%THD	θ_1	θ_2	θ_3	%THD	θ_1	θ_2	θ_3	%THD
1	50	50	53	11.87	27.93	56.76	12.56	11.66	28.18	56.69	12.60	11.95	27.59	56.61	12.66
2	50	52	51	11.25	28.83	57.28	12.41	11.00	28.47	57.48	12.49	11.25	28.88	57.31	12.41
3	50	53	57	12.27	32.86	59.67	14.60	12.15	33.35	59.61	14.84	12.21	32.91	59.77	14.60
4	50	55	52	11.16	32.01	59.40	13.32	11.36	32.18	59.53	13.39	11.39	32.85	59.92	13.65
5	50	58	51	11.07	33.79	60.79	13.97	11.14	33.93	60.81	13.97	10.84	33.05	60.27	13.55
6	50	59	52	11.48	34.91	61.54	14.73	11.47	34.73	61.70	14.58	11.51	34.99	61.58	14.73
7	51	52	56	12.32	32.56	59.40	14.14	12.67	32.82	59.15	14.27	12.31	32.55	59.40	14.14
8	51	57	50	11.13	33.54	60.52	13.29	11.13	33.81	60.28	13.58	10.94	32.97	60.15	13.52
9	53	59	53	13.40	37.92	63.00	16.25	13.09	37.96	63.02	16.36	14.41	39.50	63.78	17.77
10	54	50	53	12.49	32.45	59.06	13.41	12.62	32.28	59.13	13.41	13.13	34.56	60.21	14.28
11	58	52	50	13.53	36.52	61.34	14.28	13.63	36.25	61.40	14.33	13.25	35.87	60.98	14.26
12	56	54	50	12.96	36.04	61.42	14.00	12.94	36.15	61.54	14.26	14.05	38.24	62.58	15.60
13	55	50	53	12.82	33.50	59.58	13.72	12.71	33.76	59.67	13.78	12.66	33.75	60.01	13.84
14	50	57	54	11.83	34.44	60.96	14.84	12.12	34.39	60.92	14.93	12.61	36.08	61.89	15.83
15	50	59	52	10.71	33.05	60.38	13.74	11.68	34.69	61.69	14.58	11.48	34.91	61.54	14.73
16	51	50	56	12.31	30.82	58.34	13.63	12.62	31.07	58.14	13.74	12.32	30.86	58.36	13.63
17	51	57	54	12.30	35.33	61.42	15.18	12.90	35.61	61.15	15.48	12.93	36.57	62.09	16.09
18	51	60	59	14.15	38.41	63.00	18.47	14.80	39.13	63.58	19.24	14.73	39.30	63.41	19.20
19	60	50	54	15.32	38.96	61.92	16.35	15.11	38.66	62.15	16.10	16.28	40.76	62.58	17.57
20	59	57	50	15.22	40.70	63.74	16.91	15.20	40.66	63.92	16.93	15.47	40.92	63.89	17.24

Table 5: Number of function calls to reach the optimum value.

Run Number	PIO	PSO	GA
1	450	1900	800
2	300	1400	1400
3	450	550	750
4	400	750	850
5	350	1000	950
6	450	1250	1650
7	500	1100	1750
8	400	750	1000
9	450	950	1250
10	300	1650	1800
AVG	405	1130	1220
Avg. time taken (0.1282*Fn calls)(sec)	51.921	144.866	156.404

7 Experimental results

To validate the simulation results an experimental setup of a single-phase 7- level CHB has been developed in the laboratory and it is shown in the Figure 7. Three auto-transformers are used to vary the three different input dc voltages through the rectifiers for three bridges. The switching pulses for the switches have been generated using dSPACE ds1104 controller board, which is integrated with MATLAB. A resistive load of 100 Ω has been connected to the output terminals.

Figure 7: Experimental setup in the laboratory.

Table 6: Comparison between simulated and experimental results.

Case	V_{dc1}	V_{dc2}	V_{dc3}	θ_1	θ_2	θ_3	THD (Sim)	THD (Exp)
1	50	50	50	6.619	14.321	30.774	12.51	11.50
2	50	50	60	7.252	18.178	32.977	15.31	14.00
3	50	60	60	7.895	21.343	35.002	18.88	18.30
4	60	60	60	11.725	26.418	35.916	24.05	22.90
5	52	56	60	9.179	22.780	35.250	20.91	18.20
6	52	54	56	11.472	25.841	35.892	15.10	14.30
7	50	54	58	7.141	19.263	33.711	15.80	14.80
8	58	53	57	8.939	22.453	34.873	18.34	17.10

9	57	50	54	7.757	20.096	33.796	14.21	13.30
10	57	50	51	7.253	19.176	33.369	13.62	12.70
11	50	50	52	6.572	15.189	31.325	12.61	11.40
12	57	52	59	8.665	21.701	34.496	17.93	17.50
13	58	54	52	8.105	21.548	34.767	16.18	15.40

The results for the different input combinations are tabulated in Table 6. For each combination, the optimization has been performed in MATLAB to obtain the switching angles and the switching pulses corresponding to the switching angles have been generated through dSPACE ds1104 controller board. The experimental results for three different cases and their respective THDs are presented in Figure 8–Figure 13. From the results, it can be seen that the output voltage waveform is appearing as expected and the experimental THD values are matching with the simulated values. The experimental results for 10 different cases are summarized in the form of a Table 6. For all the given cases, the experimental results are matching with the simulated results, which validate the proposed strategy.

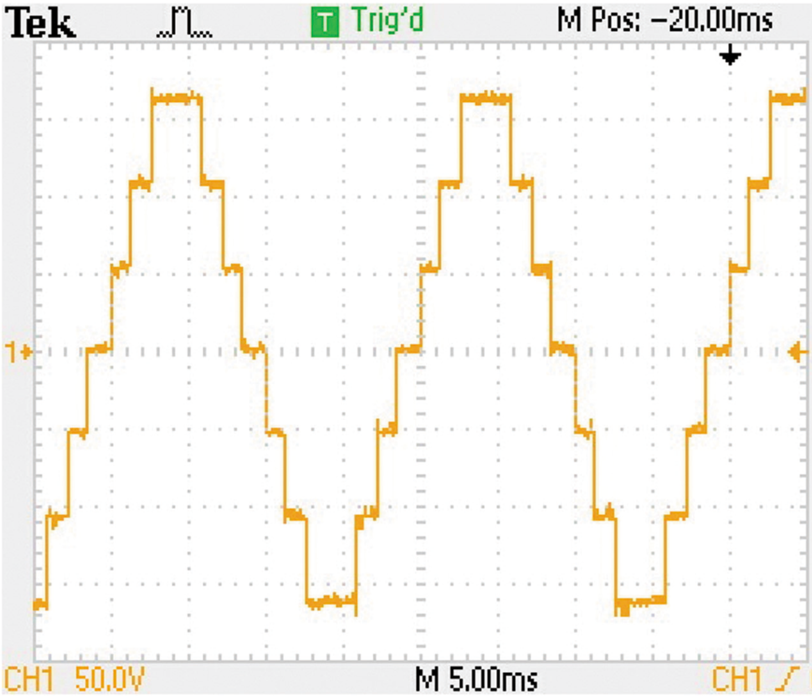

Figure 8: Output voltage waveform for V_{dc1} = 52, V_{dc2}= 54, V_{dc3} = 56.

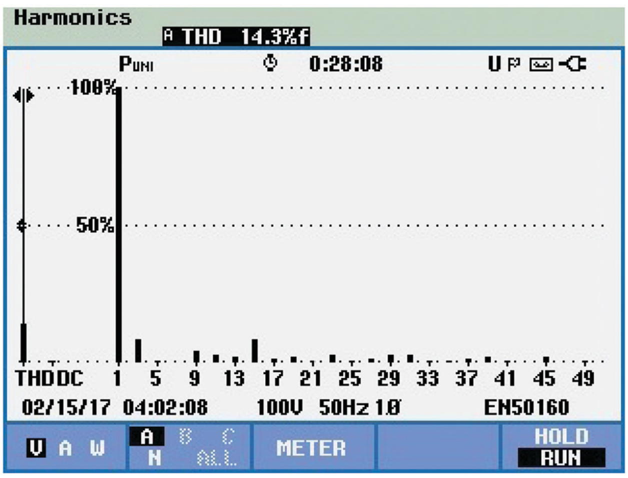

Figure 9: THD spectrum for V_{dc1} = 52, V_{dc2}= 54, V_{dc3} = 56.

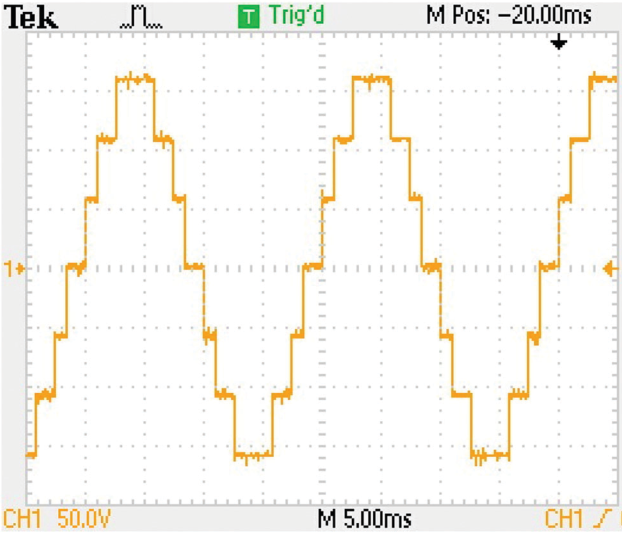

Figure 10: Output voltage waveform for V_{dc1} = 57, V_{dc2}= 50, V_{dc3} = 51.

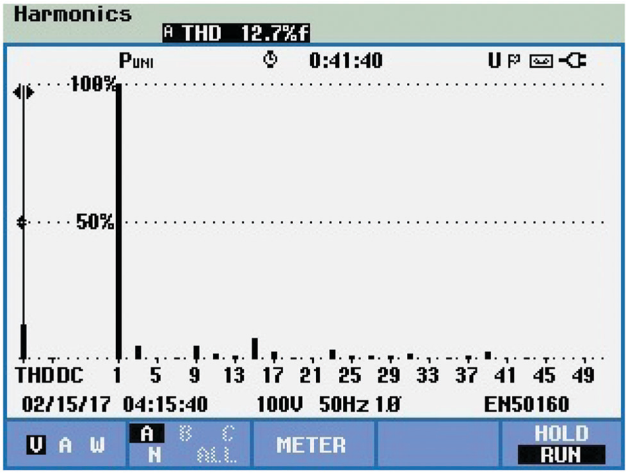

Figure 11: THD spectrum for V_{dc1} = 57, V_{dc2}= 50, V_{dc3} = 51.

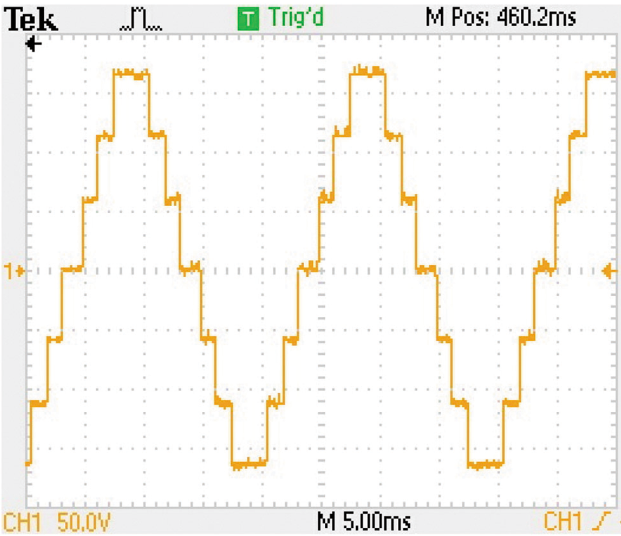

Figure 12: Output voltage waveform for V_{dc1} = 58, V_{dc2}= 54, V_{dc3} = 52.

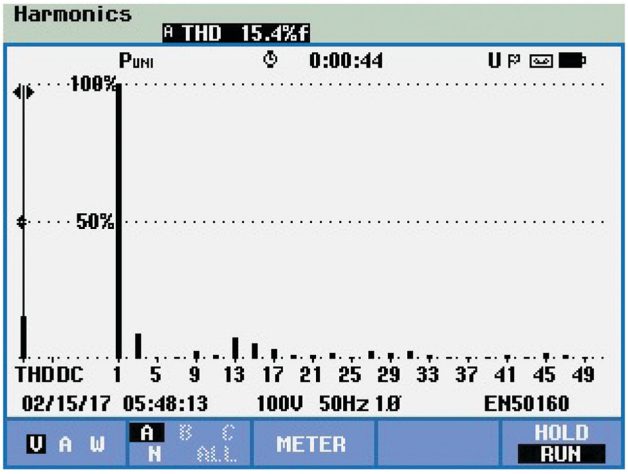

Figure 13: THD spectrum for V_{dc1} = 58, V_{dc2}= 54, V_{dc3} = 52.

8 ANN based adaptive switching angle strategy

In the proposed strategy, a two-layer feedforward neural network has been chosen with a hidden layer size of 20 neurons is as shown in the Figure 14. There are three inputs (dc voltages) and three outputs (switching angles) to the network. To generate the training data, each voltage has been varied in steps of 1 V, from 50 to 60 V, which will form the sets like [50, 50, 50], [50, 50, 51]...[60, 60, 59], [60, 60, 60]. A total of 1331 sets have been generated and the corresponding optimal switching angles have been obtained by the optimization. The parameters of the ANN are tabulated in Table 7. After the successful training of ANN with the generated data, it has been integrated with the inverter to generate switching angles to get the lowest level of THD, while maintaining the fundamental voltage constant.

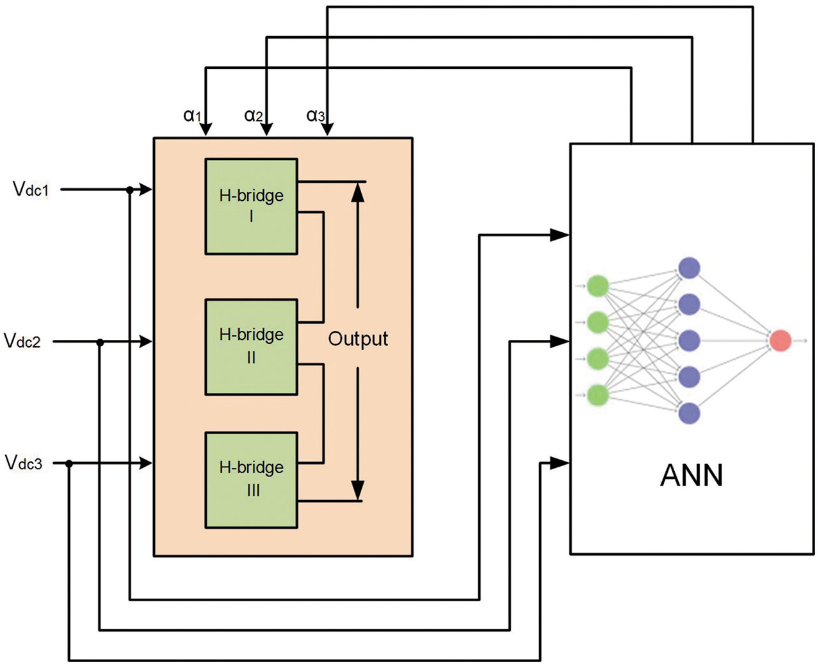

Figure 14: Proposed strategy using ANN.

Table 7: Neural network parameters.

Parameter	Value
Inputs	[V_{dc1}, V_{dc2}, V_{dc3}]

Outputs	[θ_1, θ_2, θ_3]
No. of layers	2
Size of the hidden layer	20 neurons
Training data	216 samples
Ratio of data (Training/testing/-validation)	75/15/15
Training method	Trainlm (Back-propagation)

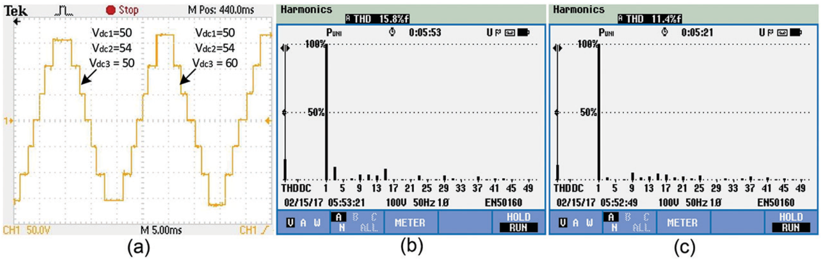

Figure 15: (a)Output voltage when the input has been changed from [50,50,50] to [50,50,60] (b) THD for [50,50,50] (c) THD for [50,50,60].

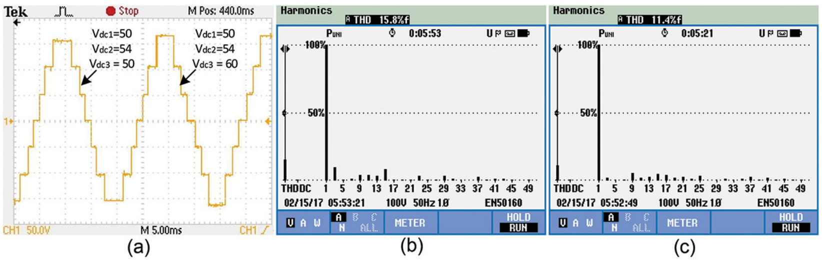

Figure 16: (a) Output voltage when the input has been changed from [50,54,50] to [50,54,60] (b) THD for [50,54,50] (c) THD for [50,54,60].

The results of the proposed strategy using ANN are shown in the Figure 15 and Figure 16. In the first result, when the input voltage has been changed from [50,50,50] to [50,50,60], the switching angles have been generated by the ANN based on the training data and can be seen in the Figure, the angles have been updated automatically. And the Figure 16 shows the output voltage variation when the input voltage has been changed from [50,54,50] to [50,54,60], which also shows that the switching angles have been adaptively changing which indicate that the ANN is able to update the firing angles with respect to the input voltage change to maintain the fundamental voltage constant while eliminating the desired order harmonics.

9 Conclusion

The harmonic minimization in the multi-level inverters is one of the many important aspects for achieving better power quality. The SHE-PWM is widely used for elimination of lower order harmonics in the literature for equal dc voltages. But, to achieve lower values of THD, when the CHB is fed with unequal dc sources a strategy has been proposed in this paper which utilizes the PIO as the optimization technique. The algorithm has been successfully implemented and validated on an experimental setup developed in the laboratory. Further, to enable the proposed strategy for real-time applications, the optimal firing angles have been trained on an ANN. The trained ANN is also able to generate optimum switching angles in real-time, making the proposed strategy suitable for PV based CHB-MLI applications.

References

[1] Portillo R, Franquelo LG, Napoles J, Leon JI, Aguirre MA. Selective harmonic elimination technique for high power converters. IEEE Trans Ind Electron. 2010;57:2315–23.

[2] Kumar J. Thd analysis for different levels of cascade multilevel inverters for industrial applications. Int J Emerging Technol Adv Eng. 2012;2:237–44.
[3] Tolbert LM, Peng FZ, Habetler TG. Multilevel converters for large electric drives. IEEE Trans Indus Appl. 1999;35:36–44.
[4] Chiasson JN, Tolbert LM, McKenzie KJ, Du Z. Elimination of harmonics in a multilevel converter using the theory of symmetric polynomials and resultants. IEEE Trans Control Syst Technol. 2005;13:216–23.
[5] Vesapogu JM, Peddakotla S, Kuppa SRA. Harmonic analysis and fpga implementation of she controlled three phase chb 11-level inverter in mv drives using deterministic and stochastic optimization techniques. Springer Plus. 2013;2:370.
[6] Aleenejad M, Ahmadi R, Moamaei P. Selective harmonic elimination for cascaded multicell multilevel power converters with higher number of h-bridge modules. In: 2014 Power and Energy Conference at Illinois (PECI), Feb 2014:1–5.
[7] Ozpineci B, Tolbert LM, Chiasson JN. Harmonic optimization of multilevel converters using genetic algorithms. In: Power Electronics Specialists Conference, 2004. PESC 04. 2004 IEEE 35th Annual, volume 5. IEEE, 2004:3911–6.
[8] Haghdar K, Shayanfar HA, Shahidi Alavi MH. Selective harmonics elimination of multi level inverters via methods of gps, sa and ga. In: Power and Energy Engineering Conference (APPEEC), 2011 Asia-Pacific. IEEE, 2011:1–5.
[9] Kavousi A, Vahidi B, Salehi R, Bakhshizadeh MK, Farokhnia N, Hamid Fathi S. Application of the bee algorithm for selective harmonic elimination strategy in multilevel inverters. IEEE Trans Power Electron. 2012;27:1689–96.
[10] Taghizadeh H, Tarafdar Hagh M. Harmonic elimination of cascade multilevel inverters with nonequal dc sources using particle swarm optimization. IEEE Trans Indus Electron. 2010;57:3678–84.
[11] Gaur P, Verma YP, Singh P. A particle Swarm optimization based switching scheme for seven-level cascaded hybrid bridge inverter, 2017:609–15.
[12] Debnath S, Ray RN, Ghosh T.. Comparison of different soft techniques applicable to multilevel inverter for harmonic elimination. *Int J Comput Appl*. 2012;6:94–104
[13] Bouhali O, Bouaziz F, Rizoug N, Talha A. Solving harmonic elimination equations in multi-levelinverters by using neural networks. Int J Inf Electron Eng. 2013;3:191.
[14] Kumar J, Gambhir J, Kumar A. Control of switching angles for a cmli using ann. In: Engineering and Computational Sciences (RAECS), 2014 Recent Advances in. IEEE, 2014:1–6.
[15] Buccella C, Cimoroni MG, Latafat H, Graditi G, Yang R. Selective harmonic elimination in a seven level cascaded multilevel inverter based on graphical analysis. In: IECON 2016-42nd Annual Conference of the IEEE Industrial Electronics Society, Oct 2016:2563–8.
[16] Yang K, Tang X, Zhang Q, Yu W. Unified selective harmonic elimination for fundamental frequency modulated multilevel converter with unequal dc levels. In: IECON 2016-42nd Annual Conference of the IEEE Industrial Electronics Society, Oct 2016:3623–8.
[17] Hajizadeh M, Fathi SH. Selective harmonic elimination strategy for cascaded h-bridge five-level inverter with arbitrary power sharing among the cells. IET Power Electron. 2016;9:95–101.
[18] Dahidah MSA, Konstantinou G, Agelidis VG. A review of multilevel selective harmonic elimination pwm: Formulations, solving algorithms, implementation and applications. IEEE Trans Power Electron. 2015 Aug;30:4091–106.
[19] Jacob T, Suresh LP. A review paper on the elimination of harmonics in multilevel inverters using bioinspired algorithms. In: 2016 International Conference on Circuit, Power and Computing Technologies (ICCPCT), March 2016:1–8.
[20] Sushnigdha G, Joshi A. Evolutionary method based hybrid entry guidance strategy for reentry vehicles. IFAC-PapersOnLine. 2016;49:339–44.
[21] Duan H, Qiao P. Pigeon-inspired optimization: a new swarm intelligence optimizer for air robot path planning. Int J Intell Comput Cybern. 2014;7:24–37.